

PREFACE

The present work was performed at the John A. Volpe National Transportation Systems Center (Volpe Center) in Cambridge, MA. The task is part of a Project Plan Agreement (PPA) between the Federal Aviation Administration Technical Center (FAATC) in Atlantic City, NJ and the Volpe Center. The PPA is entitled "Structural Integrity of Aging Airplanes."

The tasks address probability of crack detection and aircraft systems reliability. In doing so, they combine the results of several facets of the FAATC Aging Aircraft Program. The purpose of these tasks is to develop tools to assess the suitability of various methods for determining crack growth, residual strength, probability of crack detection, and the damage tolerance of transport aircraft.

The authors wish to thank Dr. Michael Basehore, Dr. Chris Smith, and Mr. Chris Seher of FAATC for their contributions to and support of this effort.

EXECUTIVE SUMMARY

This report describes three tasks related to probability of crack detection (POD) and aircraft systems reliability. All three consider previous work in which crack growth simulations and crack detection data in the Service Difficulty Report (SDR) database were used to estimate the in-service POD. The first task compared the POD estimates with estimates obtained from other sources. The second task assessed the self-consistency of the estimated POD and the crack growth simulation. The third task integrated the POD estimates with crack growth data and residual strength models to assess the cumulative probability that damage will be detected as a function of loss in residual strength.

One simulation employed in the previous work assumed single cracks growing in an infinitely wide plate. No effects of rivet holes or supporting structures were considered. The other simulation used various models to account for multiple crack initiation, load redistribution, rivet interference, and crack linkup. The POD estimates generated with the single crack growth assumption predicted lower POD for all cracks. The multiple crack methodology exhibited much better agreement with the independent estimates.

Self-consistency was measured by comparing the cumulative distributions of detected cracks of crack growth and inspection simulations to that of the actual data. Each simulation was run numerous times. Simulated inspections were performed at appropriate intervals. Random numbers were compared to the estimated POD to determine whether cracks were detected. Various assumptions were made regarding the effect a crack detection would have on the search for neighboring cracks. Once again, the simulations that allowed for the formation and linkup of multiple cracks provided the best correlation with the field data. Of those, the one that assumed a detection would induce sufficient diligence to find all nearby cracks performed best. An attempt to determine a "background" level of nondetection for large cracks was unsuccessful because of the inherent "noise" in the SDR data. Properly accounting for the influence of detections in neighboring bays could bring the distribution even more in line with the SDR data.

The reliability estimates were based on flat panel lap joint specimens. Reliability was characterized in terms of the cumulative probability that damage would be found as a function of the resulting loss in residual strength. The residual strength was calculated for the specimens using a net section yield approach. The cumulative POD was estimated by calculating the combined probability that all cracks were missed at all inspections up to that point. Two inspection methods and three inspection intervals were investigated. This approach can be extended to more advanced growth data and failure models.

TABLE OF CONTENTS

1. INTRODUCTION 1

2. COMPARISON OF THE POD CURVES TO INDEPENDENT ESTIMATES 5

3. SELF-CONSISTENCY OF THE POD ESTIMATING PROCESS 8

 3.1 SIMULATIONS OF THE CRACK GROWTH AND INSPECTION PROCESS .. 8

 3.2 INDEPENDENCE OF DETECTION OF NEIGHBORING CRACKS 9

 3.3 BACKGROUND NONDETECTION LEVEL 10

 3.4 RESULTS AND DISCUSSION 10

4. RELIABILITY ESTIMATES 14

 4.1 DESCRIPTION OF ANALYSIS AND METHODOLOGY 14

 4.1.1 Data for Distribution and Growth of
 Multiple Cracks 14

 4.1.2 Residual Strength Calculation 14

 4.1.3 Probability of Crack Detection 18

 4.2 DISCUSSION 23

5. CONCLUSIONS 30

REFERENCES 31

LIST OF FIGURES

Figure	Page
1.1 Schematic of Detection and Nondetection Events	2
1.2 Comparison of POD Curves from Two Different Methodologies	4
2.1 Comparison of Derived POD Curves with Independent Estimates	6
3.1 Cumulative Distribution of Detected Cracks from Simulations Using Weibull Probability Density Functions	11
3.2 Cumulative Distribution of Detected Cracks from Simulations Using Log Logistic Probability Density Functions	12
4.1 Schematic of Technical Framework	15
4.2 Lap Splice Panel Used in Arthur D. Little Fatigue Tests	16
4.3 Baseline Fatigue Data from ADL Fatigue Tests	17
4.4 Residual Strength Versus Number of Cycles Derived from Flat Panel Data	19
4.5 Assumed POD Curves	20
4.6 Cumulative POD versus Residual Strength for C-Check Inspections Based on ADL Panel Data WITHOUT Corrosion	24
4.7 Cumulative POD versus Residual Strength for C-Check Inspections Based on ADL Panel Data WITH Corrosion	25
4.8 Cumulative POD versus Residual Strength for Eddy Current Inspections Based on ADL Panel Data WITHOUT Corrosion	26
4.9 Cumulative POD versus Residual Strength for Eddy Current Inspections Based on ADL Panel Data WITH Corrosion	27

LIST OF TABLES

Table	Page
4.1 Information Required to Calculate Cumulative POD and Residual Strength at First Observation of Cracks	21
4.2 Residual Strength and Cumulative POD at Different Cycles ..	22
4.3 Cumulative POD for Eddy Current Inspection 4500 Cycle Inspection Interval	23

1. INTRODUCTION

As aircraft age, they become more susceptible to service related damage such as multiple cracking. The damage tolerance philosophy of aircraft design states that, should "serious" damage occur, an aircraft must be capable of safe operation until the damage is detected [1]. If undetected multiple cracks grow in size and density, the structure may no longer meet its damage tolerance requirements with respect to other damage (e.g., discrete source damage). When multiple cracks reach this stage, they are referred to as Widespread Fatigue Damage (WFD).

Two fundamental questions regarding the influence of WFD on structural integrity are: (1) For a structure containing a given configuration of multiple cracks, what is its residual strength? (2) At what rate does the degradation of strength occur? The answers to these questions are being investigated through current research project initiatives which entail both analytical and experimental studies. Once these fundamental questions have been answered, the challenge is to integrate the research results into a unifying framework that would be useful to make informed decisions regarding rule-making.

Damage tolerance for fatigue depends on the detection of damage before it progresses to the point of WFD. Fatigue damage is usually found through nondestructive inspection (NDI) which includes visual, eddy current, or ultrasound. Therefore, the probability of crack detection (POD) for NDI is necessary for an appropriate damage tolerance assessment. POD is a strong function of crack size and inspection method. Moreover, POD curves are difficult to accurately quantify for cracks less than 0.5 inches long which, unfortunately, is an important range for WFD cracks.

Classical attempts to characterize POD usually involve laboratory or field tests of equipment and methodologies under various conditions. However, an alternative approach was considered in Reference 2. Cracks that were detected during maintenance operations were analyzed to estimate their sizes during previous inspections, as shown in Figure 1.1. From these detection and nondetection events, after appropriate restrictions of the data, the maximum likelihood method was used to estimate the probability of detection as a function of crack size. The estimates of POD relied on several assumptions, ranging from the veracity of the elements of the crack growth models to the fidelity of the crack detection data in the Service Difficulty Report (SDR) database.

Two methods were used to calculate the size history of the detected cracks. The first involved the nominal crack growth histories obtained from a computational simulation of initiation, growth, and linkup of cracks in a typical fuselage bay [2]. The

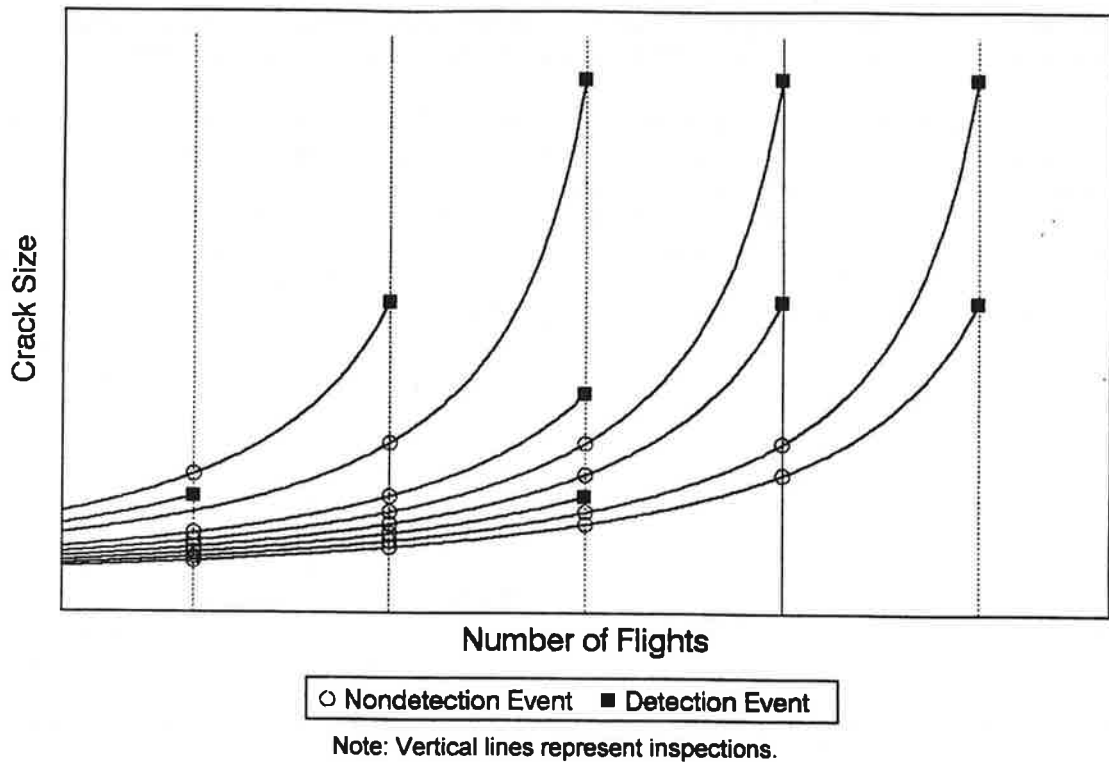


Figure 1.1. Schematic of Detection and Nondetection Events.

second was a single crack growth model using the parameters for a Walker crack growth model recommended in the Damage Tolerance Handbook [3]. The two methodologies produced significantly different estimated POD curves, regardless of the probability distribution function (PDF) assumed. Figure 1.2 illustrates the difference between the curves based on the log logistic PDF.

There are three main objectives of the present report. The first is to compare the estimated POD curves to other, independent estimates. The second purpose is to ascertain the extent of self-consistency of the estimates. That is, if the data, crack growth, and POD models were accurate, then simulations of the processes should produce data with a similar distribution to the field data. The trends are best depicted by the cumulative distribution of detected cracks (the fraction of total detected cracks that are at or below a given crack size). The third purpose is to describe a methodology which combines the results from the structural integrity and reliability research areas to create a unifying framework. Example calculations are given to illustrate the procedure of the analysis. The output of the analysis is a quantification of the probability of detection for various levels of residual strength in the fuselage lap splice at different inspection intervals.

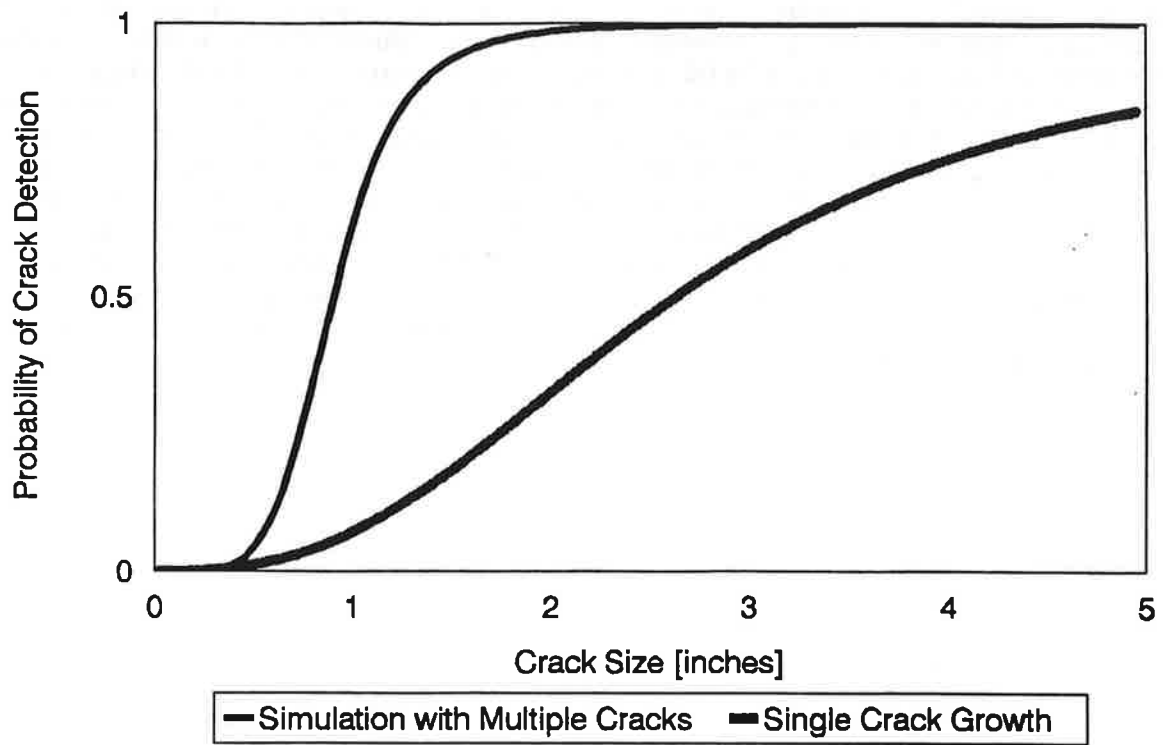


Figure 1.2. Comparison of POD Curves from Two Different Methodologies.

2. COMPARISON OF THE POD CURVES TO INDEPENDENT ESTIMATES

The two POD curves shown previously in Figure 1.2 were derived from the same crack detection data but using different assumptions of how cracks grow. The data were obtained from the SDR database and were based on crack detections during C-check inspections. One curve was derived using the nominal crack growth methodology that contains stochastic elements in modeling crack initiation and growth. The methodology also addresses the linkup of multiple cracks. It should therefore be more representative of a configuration susceptible to cracking at multiple locations. The other curve was derived from the single crack methodology that specifically excludes the possibility of multiple cracking. A comparison between these two curves and some independently derived POD curves should suggest which crack growth assumption is more valid.

Since the primary inspection method in C-checks is visual, the estimated curves were compared with two independently derived visual inspection POD curves. The first curve is mentioned in a paper by Sampath and Broek [4]. The second is from Asada et al. [5]. Unfortunately, the derivation methods for these curves are not available. The first follows the trend of data in a US Air Force POD experiment ("Have Cracks - Will Travel"). The second set is likely to have been inferred from in-service crack detection data. That data would have to be manipulated in a similar manner to the way the SDR data was manipulated in Reference 2. Correlation between a POD curve from Reference 2 and the POD curve from Reference 5 may indicate nothing more than the likelihood that the same basic assumptions were used. Nonetheless, the data in Reference 5 is primarily from Boeing 747's. These aircraft should have a different propensity for multiple crack formation than Boeing 737's.

A comparison of the four POD curves is shown in Figure 2.1. The independent POD estimates of References 4 and 5 most closely match the curve from Reference 2 that is derived assuming multiple crack formation. The implication is therefore that a methodology assuming stochastic multiple crack formation and appropriate crack linkup will yield better POD estimates.

A close look at Figure 2.1 reveals that, although three POD curves (Reference 2 simulation with multiple cracking, Reference 4, and Reference 5) have similar characteristics, they could give quite different results in damage tolerance analyses. All three show a rapid rise in POD at a crack size less than an inch. The location of this rise might be considered an approximate threshold detection size. The differences in these threshold values could imply significant differences in the ability to detect a crack before it reaches a dangerous size. For example, the probability of detection of a 0.6" crack for the

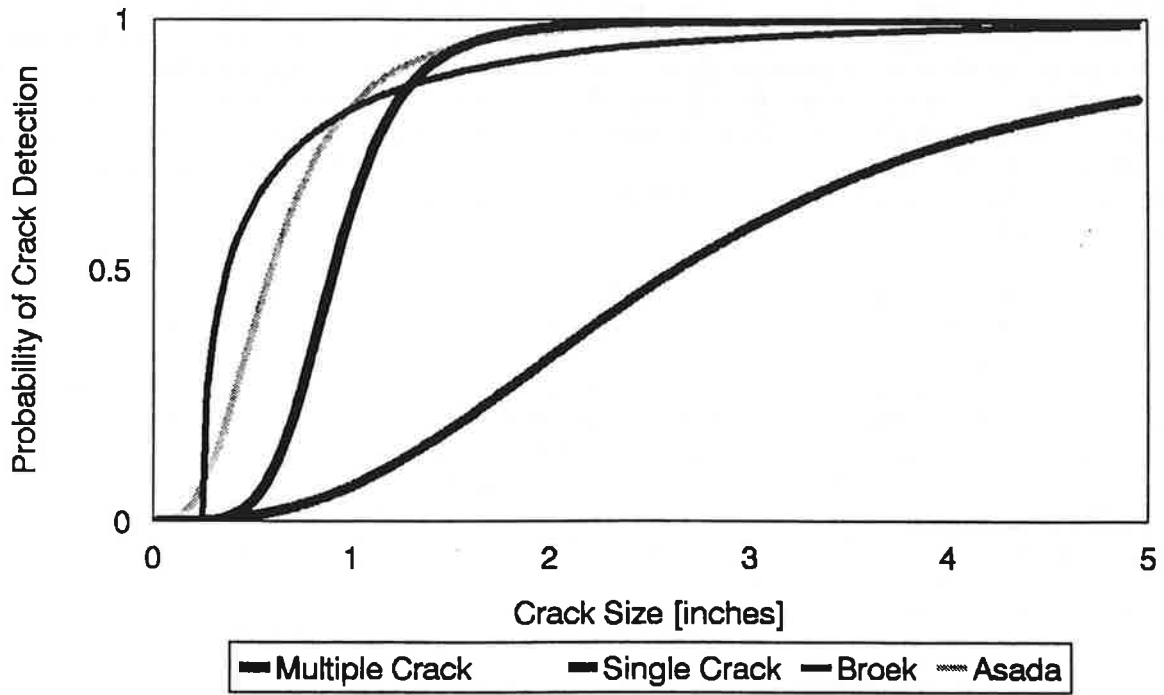


Figure 2.1. Comparison of Derived POD Curves with Independent Estimates.

three curves are approximately 10%, 70%, and 50%, respectively. Depending on the speed with which the multiple cracks link up, the cumulative probability of detecting a crack before it becomes dangerous could be severely affected. Thus, these curves, though similar, should not be used interchangeably.

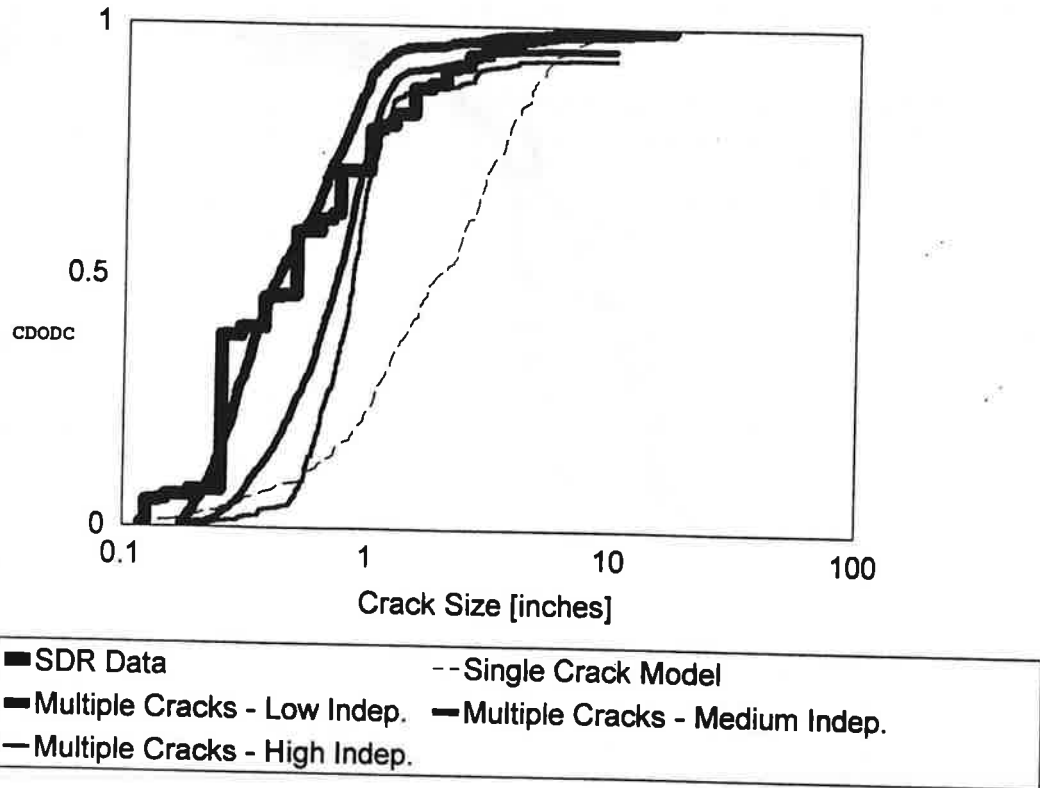


Figure 3.2. Cumulative Distribution of Detected Cracks from Simulations Using Log Logistic Probability Density Functions.

The simulations that allowed for multiple cracks seemed to approximate the data more closely. Within those models, the simulations that assumed lower degrees of independence of POD matched the trend of the data better. This is consistent with instances in the database of several cracks of approximately the same size being found near each other during the same inspection. Also, the simulations assuming log logistic POD distributions performed marginally better at low crack sizes than those assuming Weibull POD distributions.

One disturbing aspect of the cumulative distributions of detected cracks is the fraction of cracks predicted to be undetected even at a crack size exceeding the width of one bay. The most plausible explanation for this deficiency is that the simulation does not allow for any dependence of POD on crack detections in neighboring bays. In fact, an inspector that finds a crack in one bay may well have a heightened awareness level while inspecting neighboring bays. A visible repair may raise awareness for neighboring bays. Thus, dependence of POD on crack detections in neighboring bays could decrease the probability of a large crack not being detected.

The POD for visual inspection and the POD for C-checks are probably not identical. Visual inspection POD estimates may include the assumption of 100% close visual inspection. In actual C-checks, however, the proximity of the inspector may vary significantly. Thus, the C-check POD might be lower than the visual POD. On the other hand, C-check inspections might include supplementary techniques when a crack is suspected. Thus, under certain circumstances, the C-check POD may be higher (or, at least, less error prone) than the visual POD alone.

4. RELIABILITY ESTIMATES

4.1 DESCRIPTION OF ANALYSIS AND METHODOLOGY

The methodology to determine the probability of detection for various levels of residual strength requires three inputs:

- (1) distribution and growth rate of multiple cracks,
- (2) residual strength as a function of crack distribution at any time or number of flight cycles, and
- (3) probability of crack detection curves.

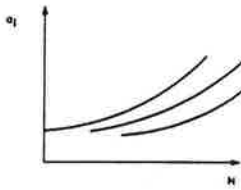
The schematic diagram in Figure 4.1 shows a framework that combines these three input elements to produce a plot of cumulative probability of detection versus residual strength for a given inspection procedure and different intervals of inspection.

4.1.1 Data for Distribution and Growth Rate of Multiple Cracks

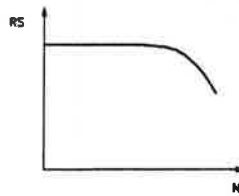
Fatigue tests have been conducted by Arthur D. Little, Inc. (ADL) using flat lap splice panels to investigate the formation and growth of multiple cracks. The ADL flat panels resemble a single bay between two tear straps in an aircraft fuselage. Figure 4.2 shows the dimensions of the panels used in these tests. A total of eight specimens were tested. Six of those contained pre-existing corrosion to determine its effect on fatigue life. All tests were performed with a maximum stress of 16 ksi, and a ratio of minimum to maximum stress of 0.1. The crack sizes in these tests were carefully observed, recorded, and subsequently reported in the open literature [6]. Figure 4.3 shows the crack growth rate observed in the two tests without pre-existing corrosion.

4.1.2 Residual Strength Calculation

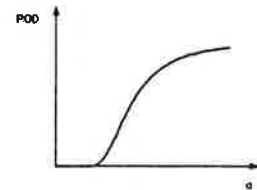
For simplicity, a global net-section yield criterion was used to estimate the residual strength of the ADL flat panels at different instances of time. Mathematically, this criterion can



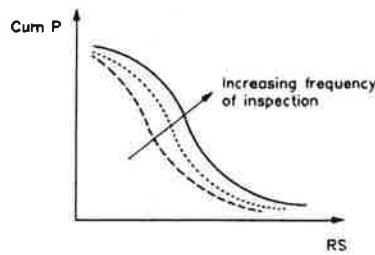
(a) Distribution and growth of multiple cracks.



(b) Residual strength versus number of cycles.



(c) Probability of detection versus crack size; also a function of inspection method



(e) Cumulative probability of detection versus residual strength for different inspection intervals; derived from (a), (b), and (c).

Figure 4.1. Schematic of Technical Framework.

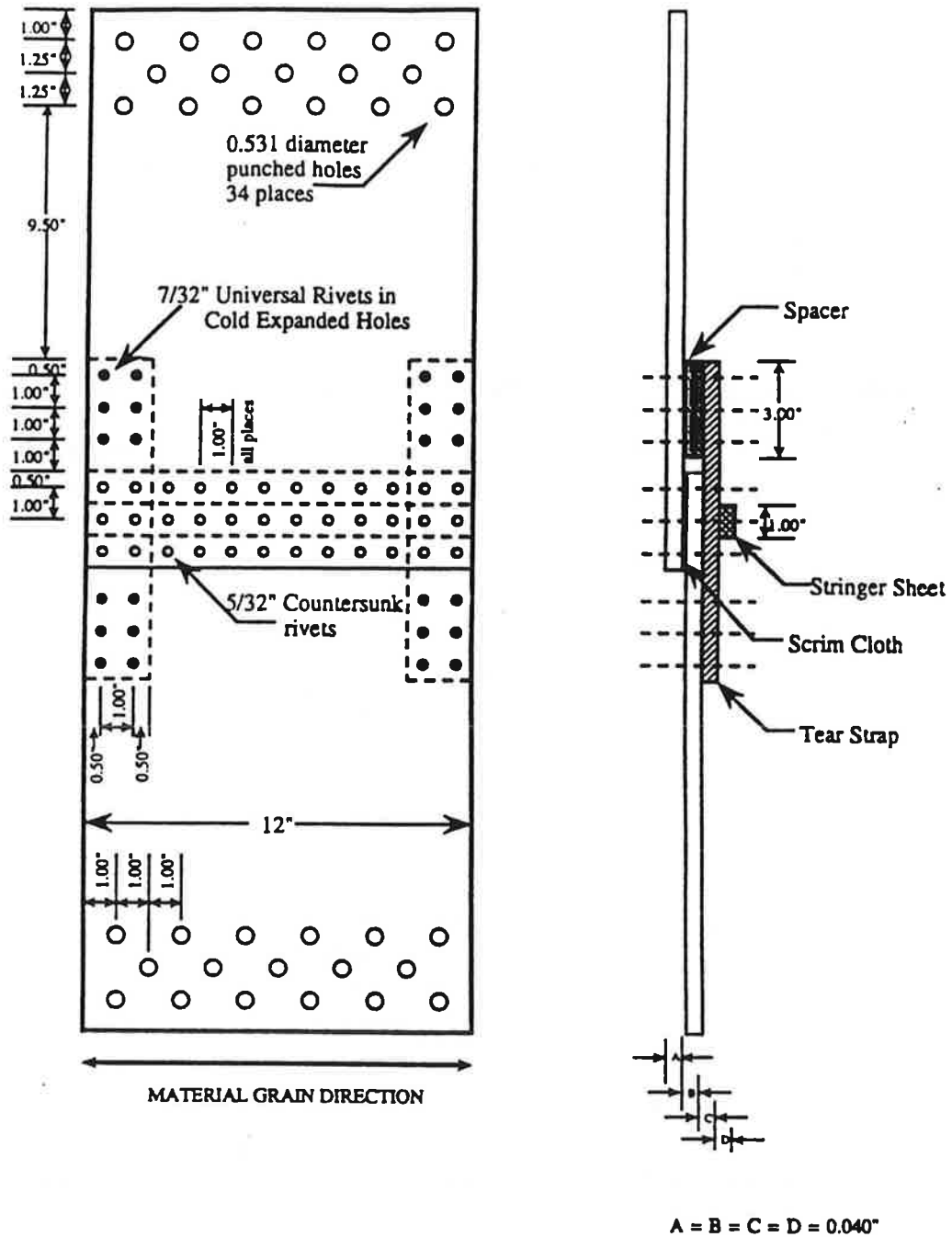


Figure 4.2. Lap Splice Panel Used in Arthur D. Little Fatigue Tests.

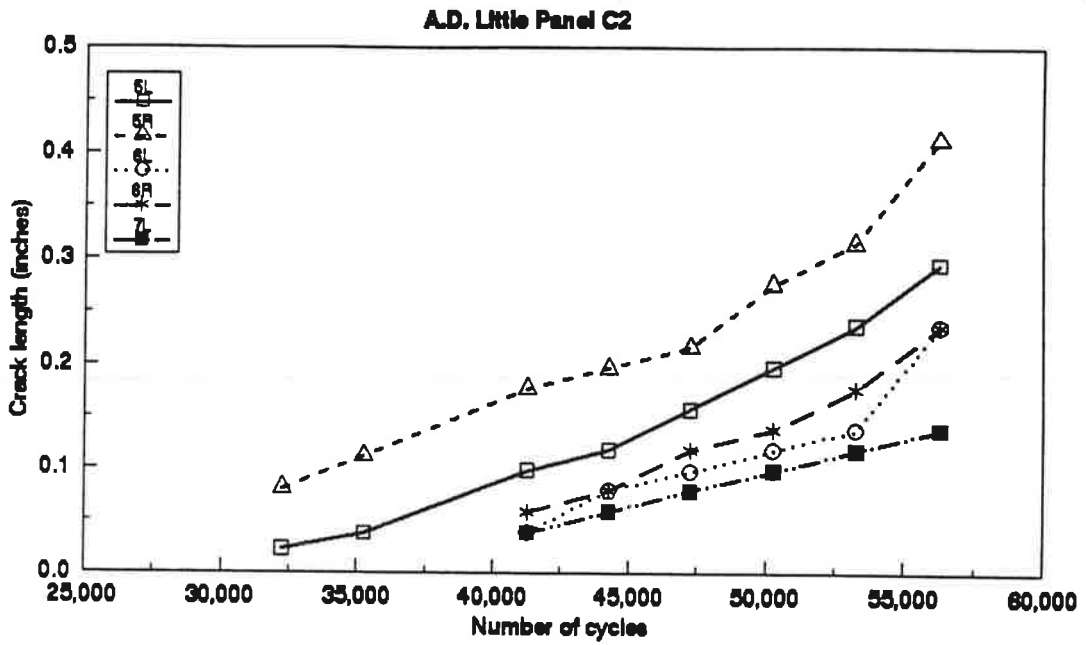
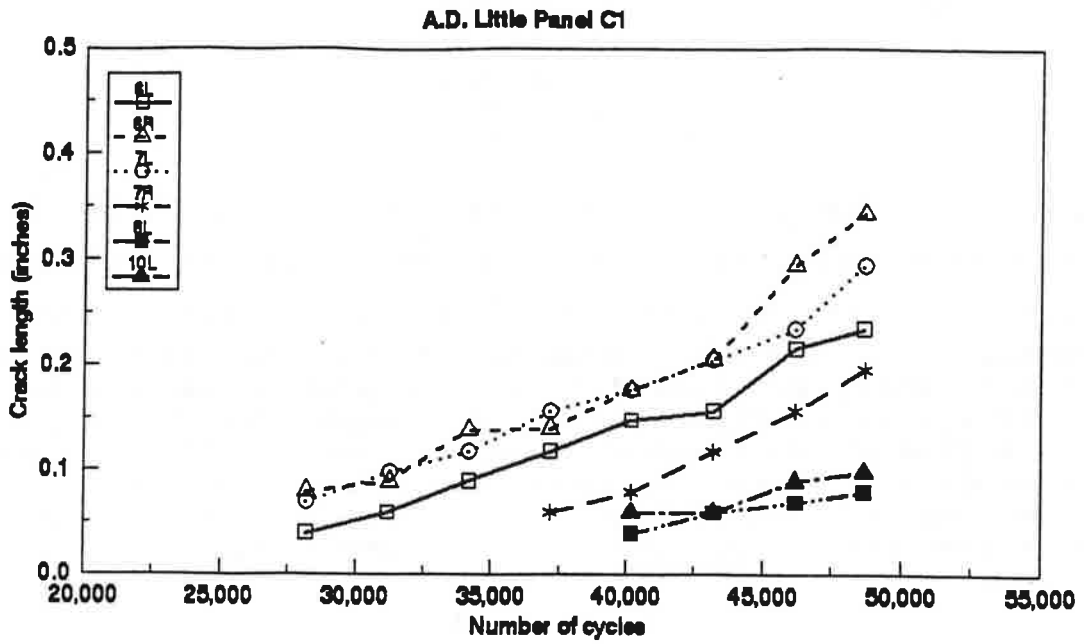


Figure 4.3. Baseline Fatigue Data from ADL Fatigue Tests.

be expressed as:

$$\sigma_R = \sigma_Y \cdot \frac{W - \sum a_i - \sum d_j}{W - \sum d_j} \quad (4.1)$$

where σ_R is the yield strength of the material, W is the width of the panel (12 inches), $\sum d_j$ is the sum of all the rivet hole diameters (1.875 inches), and $\sum a_i$ is the sum of all crack lengths. The residual strength of the ADL flat panels was estimated using equation 4.1, and is plotted as a function of applied cycles in Figure 4.4. For comparison, the figure also shows a theoretical residual strength curve for the same panel if it contained a single center-crack. The single crack curve was derived by assuming global failure by plastic collapse in conjunction with a Paris/Walker crack growth equation [7]:

$$\frac{da}{dN} = C \frac{\Delta K^p}{1-R} \quad (4.2)$$

where ΔK is the stress intensity factor range and R is the stress ratio. Values for the crack growth parameters were assumed to be $C = 4 \cdot 10^{-10}$ and $p = 4$ where ΔK is in units of $ksi \cdot \sqrt{in}$ and da/dN is in units of inch/cycle [8].

4.1.3 Probability of Crack Detection

Two different methods of inspection were considered in this example calculation: (1) the estimated logistic POD from the multiple crack analysis of the SDR data [2] and (2) eddy current. The C-check inspections are largely based on visual observations. The mathematical form for the assumed POD curve associated with level C-check inspections is given by [2]:

$$p(a) = \frac{1}{1 + e^{(\alpha a + \beta)}} \quad (4.3)$$

where a is the total crack length, $\alpha = -5.97$ and $\beta = 5.72$. The assumed POD curve for eddy current inspection is described by [9]:

$$p(a) = 1 - e^{-\left[\frac{a - a_0}{\lambda - a_0}\right]^\gamma} \quad (4.4)$$

where $a_0 = 0.05$, $\lambda = 0.15$, and $\gamma = 0.5$. The POD curves for each method of inspection are shown in Figure 4.5. These POD curves reveal

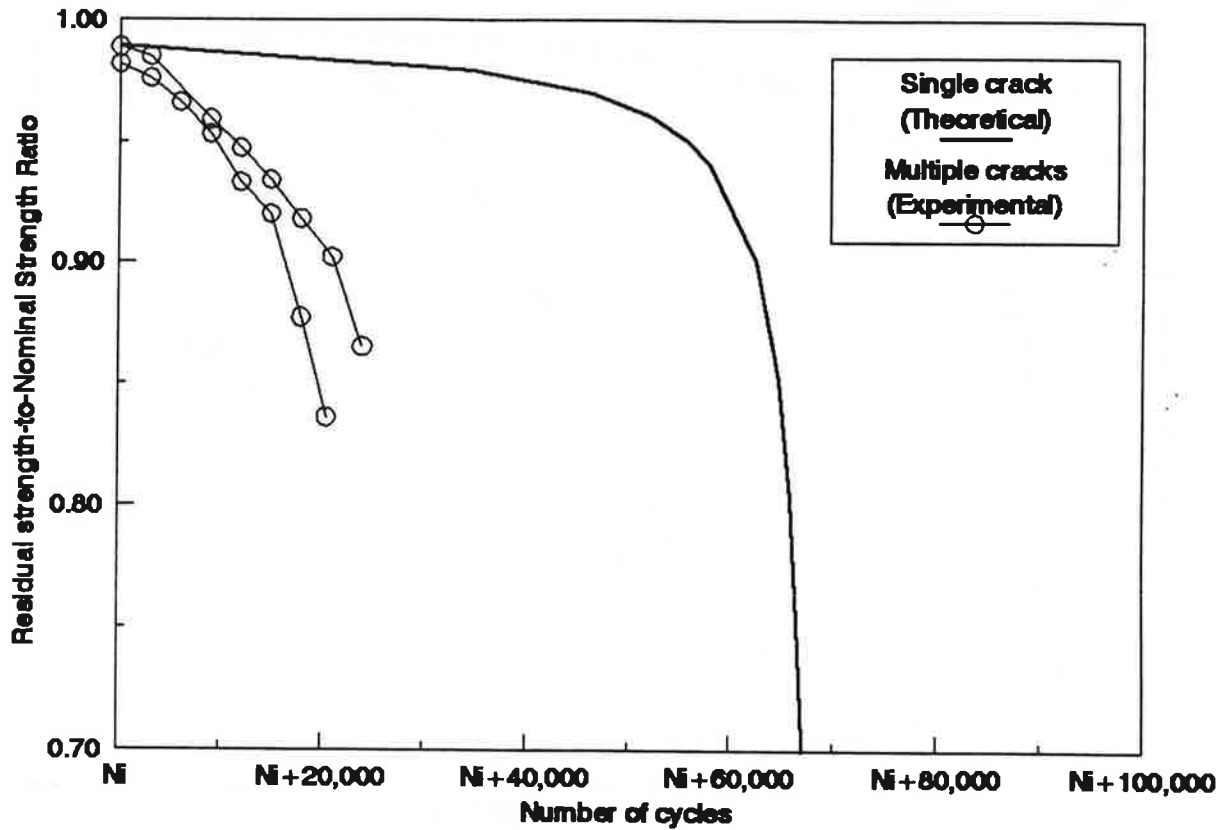


Figure 4.4. Residual Strength versus Number of Cycles
Derived from Flat Panel Data.

(Note: Ni refers to the number of cycles when cracks were first observed.)

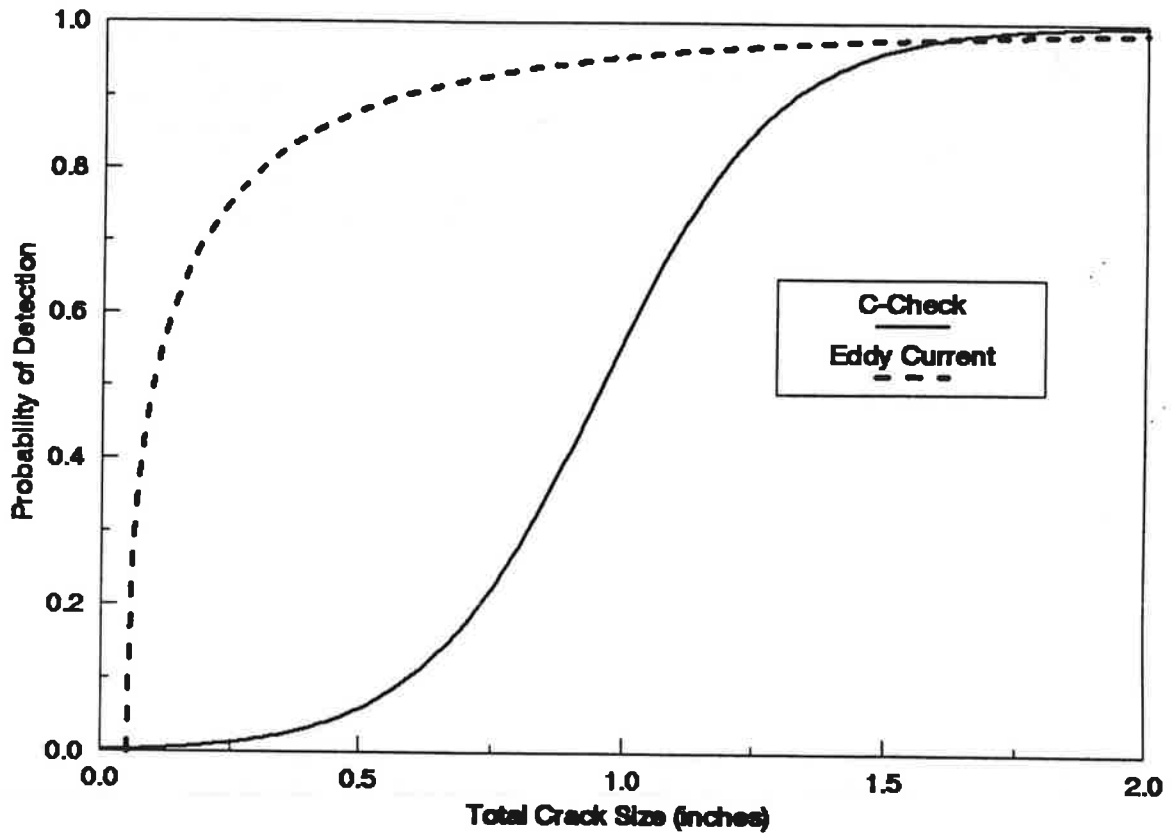


Figure 4.5. Assumed POD Curves.

that the probability of detecting cracks less than or equal to 0.5 inches is extremely sensitive to the method of inspection. For example, the POD for a 0.5-inch crack using C-check inspection is approximately 5%, while the POD using eddy current is about 85%. However, eddy current is unable to detect any cracks less than 0.15 inches according to the assumed POD curve.

In the present methodology, detection of each individual crack in a structure containing many cracks is assumed to be an independent event. In other words, the POD curve is applied to every crack in the structure separately. Table 4.1 lists crack length data from one of the ADL panel tests at the first observation of crack formation. At that instant in time, three cracks were observed. Thus, the table also includes the associated POD from equation (4.3), $p(a_i)$ and probability of non-detection, $1-p(a_i)$ for each crack.

TABLE 4.1 INFORMATION REQUIRED TO CALCULATE CUMULATIVE POD AND RESIDUAL STRENGTH AT FIRST OBSERVATION OF CRACKS

a_i [inches]	$p(a_i)$	$1-p(a_i)$
0.039	0.00412	0.99588
0.079	0.00523	0.99477
0.069	0.00493	0.99507
$\sum a_i = 0.187$	$\prod (1-p(a_i)) = 0.98579$	

Using the data in Table 4.1, the residual strength of the panel (normalized with respect to yield strength) at the given instant in time is:

$$\frac{\sigma_R}{\sigma_Y} = \frac{W - \sum a - \sum d}{W - \sum d} = \frac{12 - 0.187 - 1.875}{12 - 1.875} = 0.982 \quad (4.5)$$

The cumulative probability of detecting this particular level of residual strength is:

$$P = 1 - \prod_{i=1}^3 [1 - p(a_i)] = 1 - (0.99588)(0.99477)(0.99507) = 1 - 0.98579 = 0.01421 \quad (4.6)$$

The remaining crack growth data are used in the same manner to determine cumulative POD and residual strength at different instances in time. Results from applying this computational procedure to the ADL flat panel fatigue data are listed in Table 4.2 for the two different POD curves which implies two different inspection methods. The number of cycles in the table represents the total number of applied cycles minus the number of cycles when cracks were first observed. The results listed in Table 4.2 represent cumulative POD curves for a single inspection. Therefore, the final step of the analysis is to use

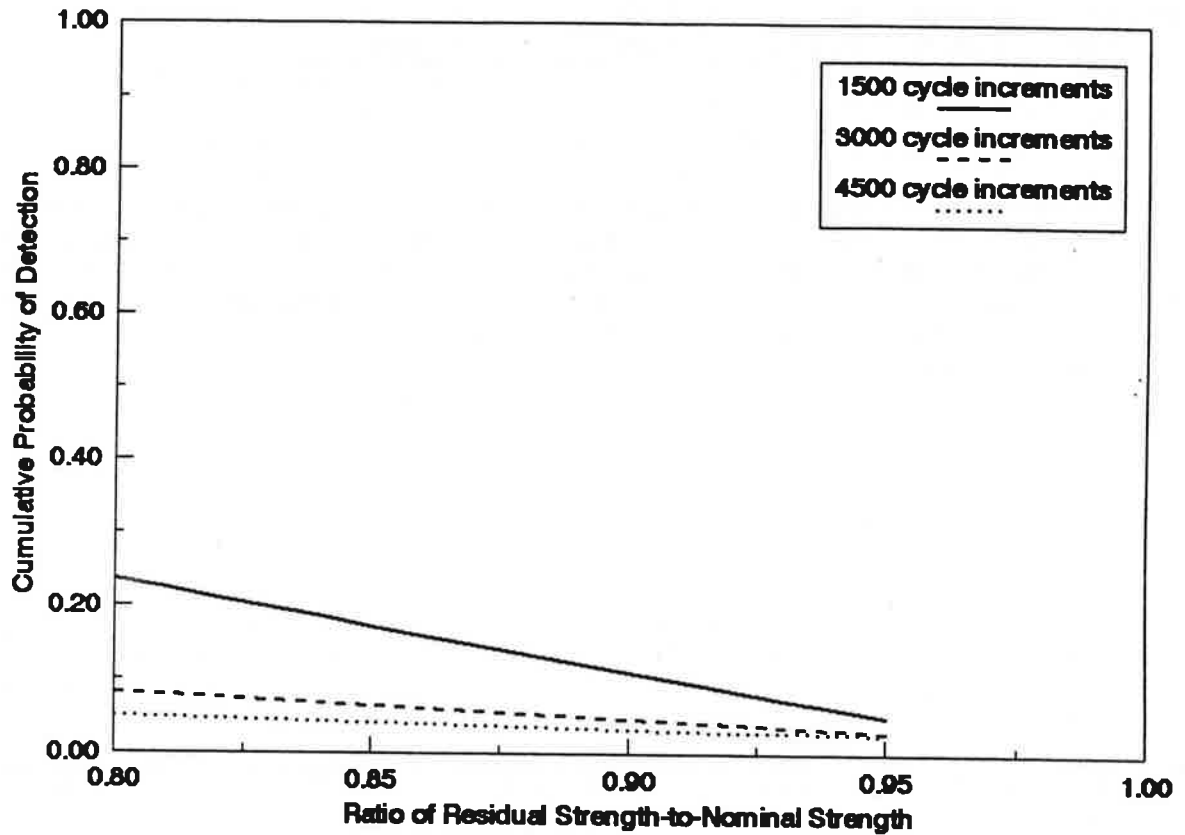


Figure 4.6. Cumulative POD versus Residual Strength for C-Check Inspections Based on ADL Panel Data WITHOUT Corrosion.

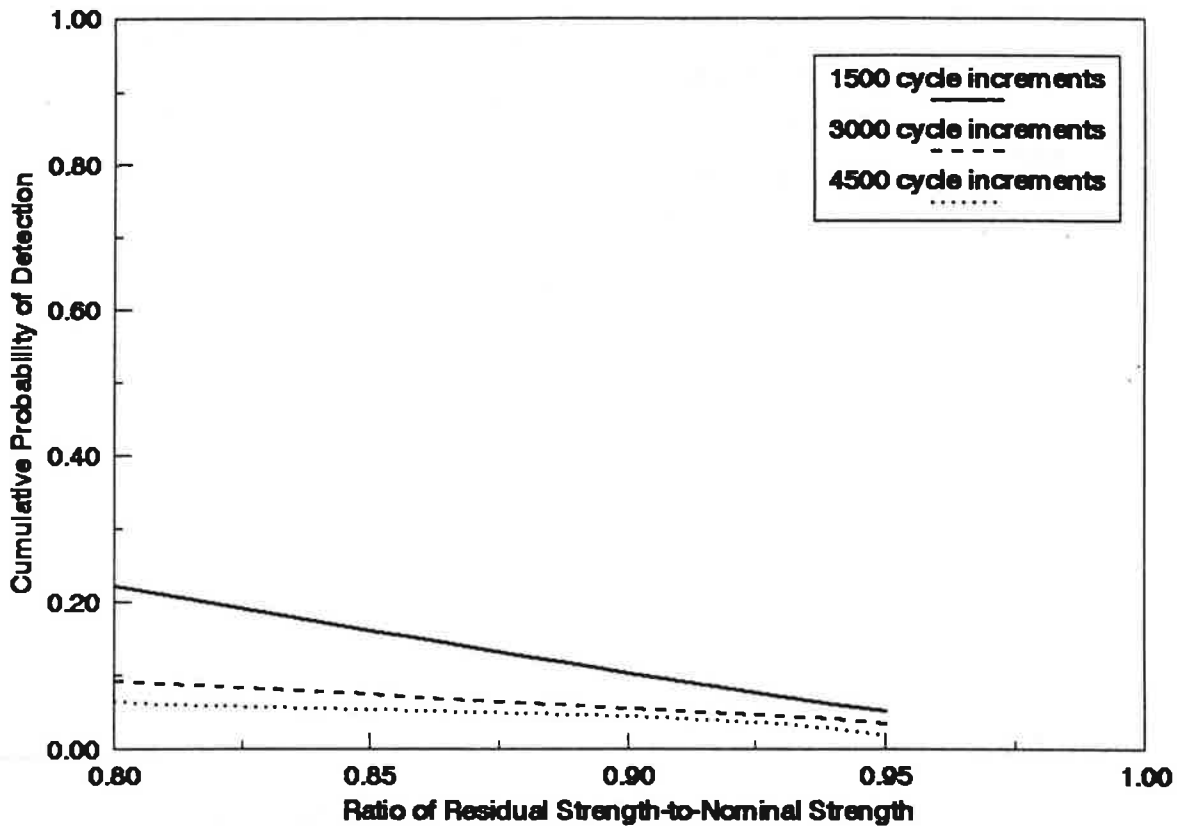


Figure 4.7. Cumulative POD versus Residual Strength for C-Check Inspections Based on ADL Panel Data WITH Corrosion.

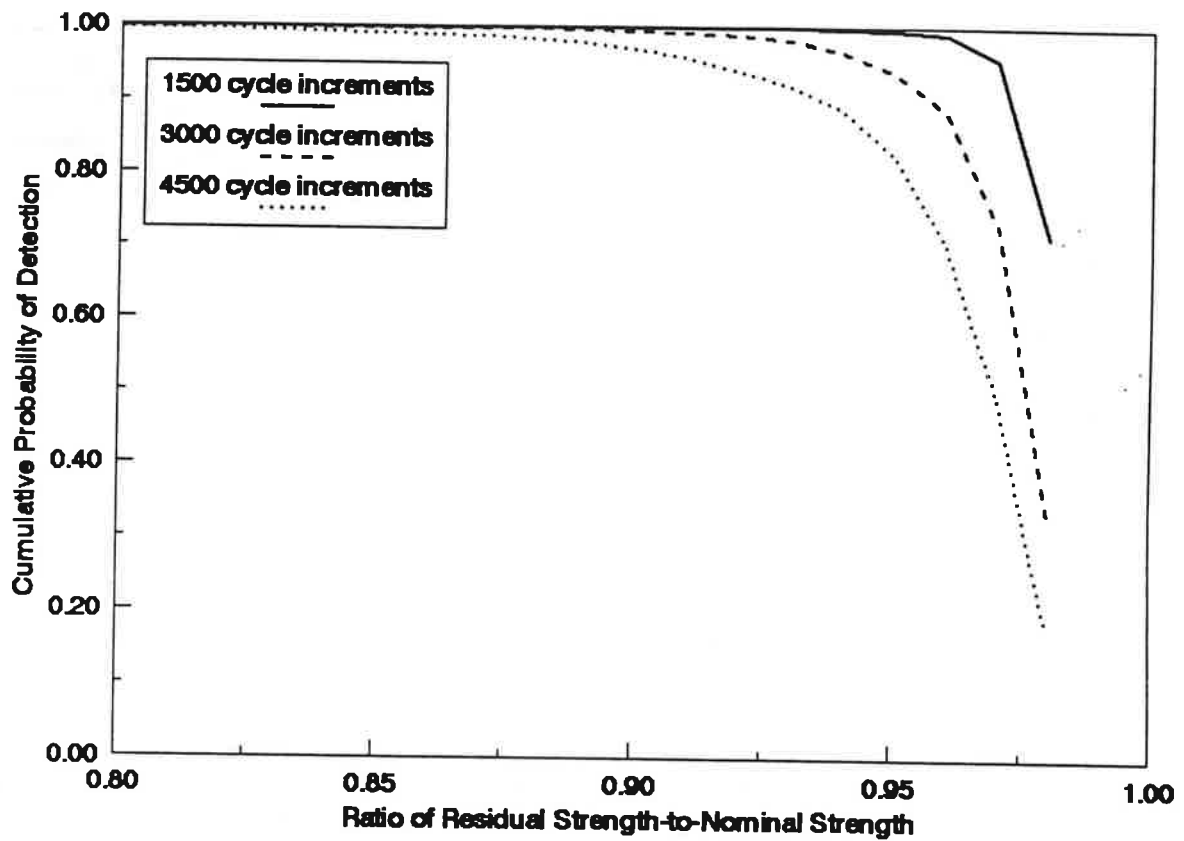


Figure 4.8. Cumulative POD versus Residual Strength for Eddy Current Inspections Based on ADL Panel Data WITHOUT Corrosion.

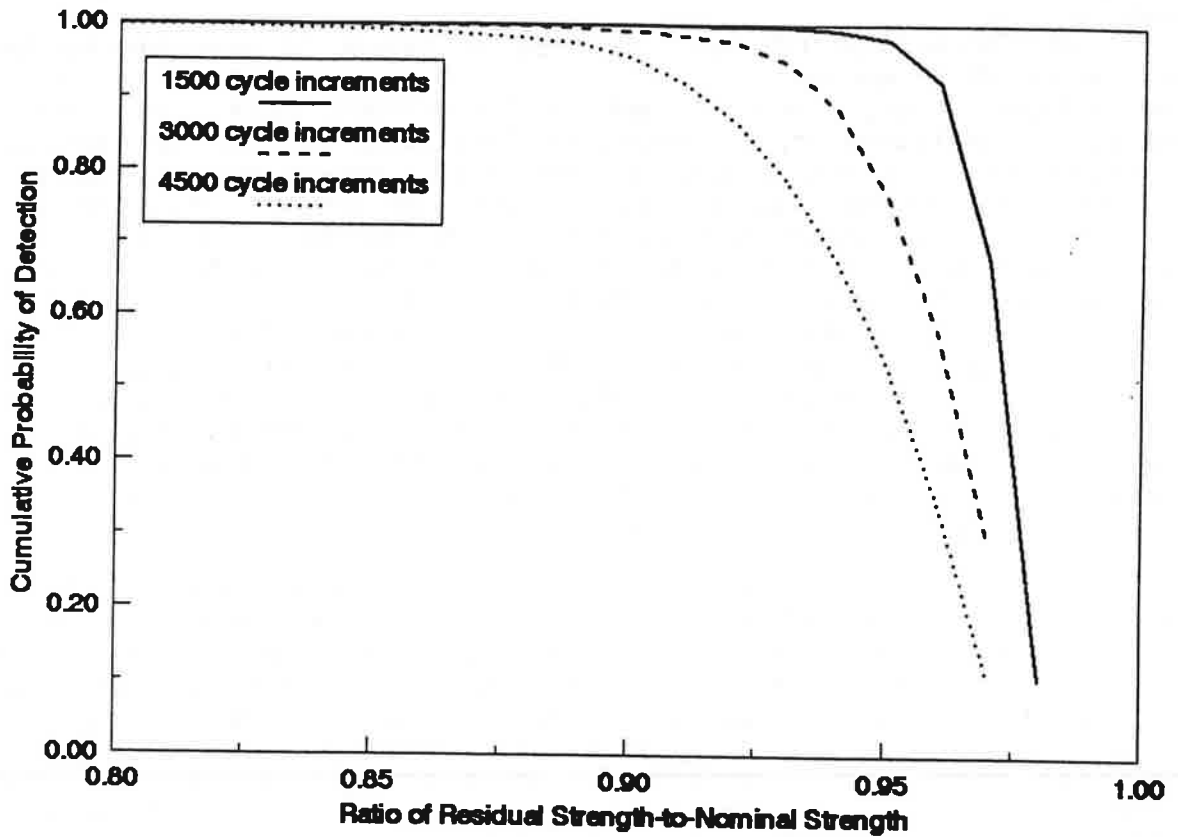


Figure 4.9. Cumulative POD versus Residual Strength for Eddy Current Inspections Based on ADL Panel Data WITH Corrosion.

12. Orringer, O., "How Likely is MSD?" Structural Integrity of Aging Airplanes, Proceedings of the International Symposium on Structural Integrity of Aging Airplanes, Springer-Verlag, Berlin-Heidelberg, 1991, pp. 275-292.